CRYSTAL GROWTH & DESIGN

Communication

pubs.acs.org/crystal

Facile Nanotube-Assisted Synthesis of Ternary Intermetallic Nanocrystals of the Ferromagnetic Heusler Phase Co_2FeGa

Markus Gellesch,[†] Maria Dimitrakopoulou,[†] Maik Scholz,[†] Christian G.F. Blum,[†] Michael Schulze,[†] Jeroen van den Brink,[†,‡] Silke Hampel,[†,*] Sabine Wurmehl,[†,§,*] and Bernd Büchner[†,§]

[†]IFW Dresden Leibniz-Institut für Festkörper- und Werkstoffforschung, 01069 Dresden, Germany

[‡]Institut für Theoretische Physik, Technische Universität Dresden, 01062 Dresden, Germany

[§]Institut für Festkörperphysik, Technische Universität Dresden, 01062 Dresden, Germany

Supporting Information

ABSTRACT: A facile synthesis approach for the synthesis of ternary intermetallic nanocrystals was demonstrated exemplarily with the Heusler compound Co_2FeGa. The method, involving prefabricated multiwalled carbon nanotubes which act as a template and protective shell, results in the formation of mainly spherical, chemically stable, and crystalline nanoparticles with a well-defined diameter distribution. As an example, for novel functionalities arising from downscaling a bulk material, we observe an enhancement of the coercive field of the Co_2FeGa nanocrystals by a factor of ≈30. Our work can facilitate the exploration and eventually the tuning of physical properties of ternary and other intermetallic compounds at the nanoscale.

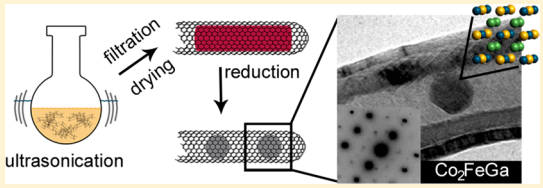

Heusler materials are a family of intermetallic compounds with the general stoichiometry of X_2YZ, where X and Y denote transition metals and Z a main group metal. They are named after Friedrich Heusler who discovered ferromagnetism in the compound Cu_2MnAl.[1,2] Nowadays more than 1300 Heusler compounds are reported in literature and their known physical properties extend well beyond the different types of magnetism and comprise, among others, magnetocaloric, thermoelectric, shape memory, half-metallic ferromagnetic, superconducting, semiconducting, and potentially topologically insulating materials.[3] Heusler materials are usually prepared as single or polycrystalline bulk materials or thin films. However, for numerous potential applications (e.g., in spintronics), the nanoscale dimensions of a material cannot be neglected.[4] When the characteristic length of a material is in the range of nanometers, finite size effects and a high surface to volume ratio strongly affect the physical properties of a material. Examples for such occurrences are ballistic transport in carbon nanotubes,[5] photoluminescence of gold nanoparticles,[6] or the enhanced catalytic activity of nanoparticles.[7] In order to investigate the effects of downscaling on a given compound, crystalline samples with nanoscale dimensions (e.g., in the form of nanoparticles or nanowires) are necessary.

A straightforward way of preparing Heusler nanoparticles is ball milling of polycrystalline starting materials.[8−10] This process, however, is rather crude as it involves high-energy input on debris of the milled material, which may lead to structural changes. Further, Heusler particles which are prepared this way are prone to oxidation and in this sense require very careful handling. A recent approach to synthesize Heusler nanoparticles was presented by L. Basit and coworkers.[11] They applied a wet chemical method which involved the precipitation of Heusler particles on a porous silica matrix. Although this method avoids the known issue of the high kinetic energies involved in ball milling processes, the control of the particle size remains poor and the synthesis requires an additional coating step to protect the nanoparticles from oxidation, which is further followed by HF etching to retrieve the particles from the silica matrix. With such drawbacks in the synthesis, the study of the physical properties of Heusler nanoparticles in a reliable manner constitutes a challenge.

In order to help overcome the limitations of the known synthesis methods, we suggest an alternative and elegant approach based on nanoparticles encapsulated inside the hollow cavity of carbon nanotubes. In our experiments, we have filled multiwall carbon nanotubes with the intermetallic Heusler compound Co_2FeGa, by extending a reported solution-filling approach for carbon nanotubes.[12]

We investigated the geometry of the filling particles and their position in respect to the carbon nanotubes with scanning electron microscopy (SEM) (Figure 1) and transmission electron microscopy (TEM). The distribution of filling particle diameters (d_{NP} = 35 ± 7 nm) measured perpendicular to the long axis of the tubes coincides with the distribution of the inner diameter of filled carbon nanotubes (d_{CNT} = 38 ± 9 nm) (Figure 2). Thus, we observe that the confinement of the intermetallic material to the inner diameter of the nanotubes allows control of the particle size.

The aspect ratio (i.e., the ratio of the long particle axis to its short axis) of the majority of the filling particles (86%) is spherical within one standard deviation in a sample of 70 filling

Received: March 19, 2013
Revised: May 21, 2013
Published: June 7, 2013

   dx.doi.org/10.1021/cg400405k | *Cryst. Growth Des.* 2013, 13, 2707−2710

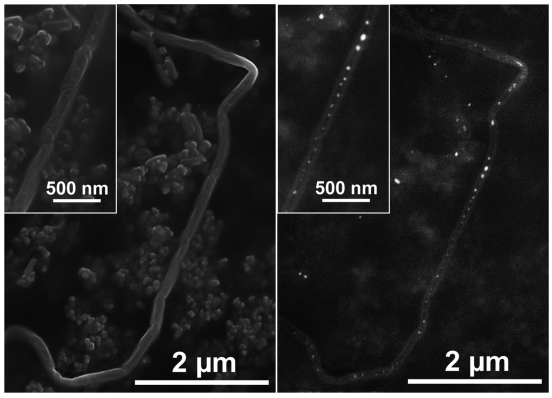

Figure 1. SEM micrographs of an individual filled carbon nanotube after the reduction process, once in topography mode [i.e., secondary electron image (left)] and the same scene with elemental contrast [i.e., back-scattered electron image (right)]. The inset shows an enlarged view of the straight middle part of the filled carbon nanotubes. Here, the "pearl-necklace"-type alignment of the nanoparticles along the inner cavity of the nanotube, as well as the separated placing of the nanoparticles, can be observed.

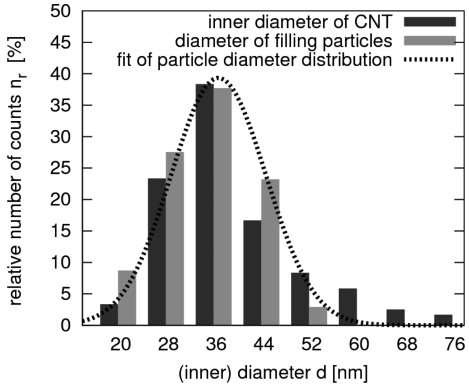

Figure 2. Histogram of the diameter of filling particles. Particle diameters were measured perpendicular to the long axis of the respective carbon nanotube. The diameter distribution of the particles follows the distribution of inner carbon nanotube diameters. A Gaussian fit of the particle diameter distribution yields a mean particle size of 35 ± 7 nm.

particles (Figure 3). Only about 5% of the particles show an aspect ratio larger than 1.5, where 1.9 constitutes the largest aspect ratio found in our samples. We attribute the primary formation of spherical particles to the minimization of surface energies during the formation of particles in the reduction process.

The samples have been exposed to air for several months; however, we find no hints for oxidation of the filling particles, even at those close to the open tips of the carbon nanotubes. This chemical stability is a significant advantage, not only over unprotected intermetallic nanoparticles, but also over Heusler thin films and bulk Heusler compounds, where battling oxidation constitutes a permanent challenge.[13,14]

We observe particles inside nanotubes positioned at varying places along the tube: they occur in the middle of tubes, as well as at the tip and in between (see Figure 1). Our samples show no significant amount of particles outside of carbon nanotubes. The virtual absence of outside particles is confirmed by thermogravimetric analysis (TGA): here, we observe a weight loss contributed to the combustion of carbon nanotubes

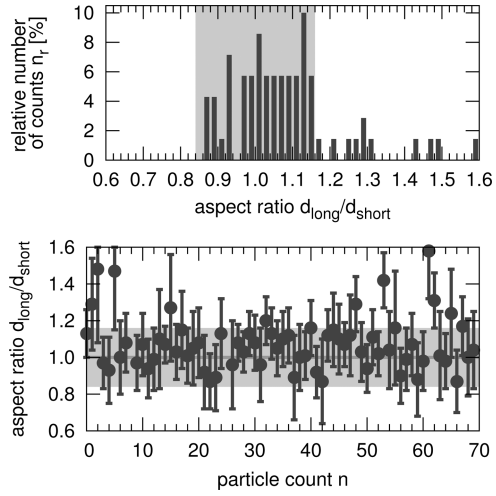

Figure 3. Aspect ratio of filling particles. The shaded areas indicate one standard deviation, and the solid line at 1.0 is a guide to the eye. Of the particles, 86% exhibit an aspect ratio of 1.0 within one standard deviation and, thus, are mostly spherical. Only a few particles (below 5%) show an aspect ratio larger than 1.5.

(Figure 3) and no additional features in the data curve. In contrast to our here discussed samples, other samples of filled carbon nanotubes with numerous outside particles (confirmed with SEM and TEM), exhibit an increase in mass prior to the combustion of the carbon nanotubes (Figure 4). We attribute

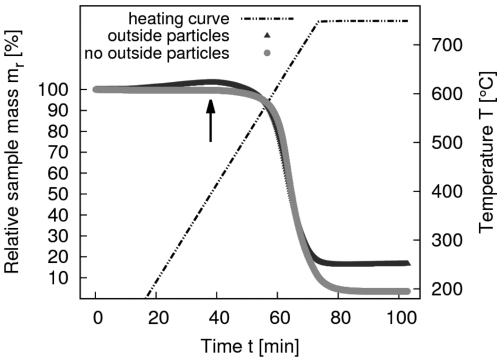

Figure 4. Sample purity as examined by thermogravimetric analysis: filled carbon nanotubes with a large amount of outside particles show a mass increase (arrow) prior to the combustion of the carbon nanotubes, while the here discussed samples of filled carbon nanotubes lack this specific increase in mass, which indicates the high purity (i.e., the virtual absence of outside particles, in these samples).

this increase to the oxidation of the outside particles that are no longer protected against oxidation by the contact to the outer carbon shells of the nanotubes due to the applied elevated temperature. The observation, that this specific increase in mass is not present in the here discussed samples of filled carbon nanotubes, further evidences the high sample purity. From the TGA data, we also derive a filling yield of intermetallic material of approximately 2−3 wt %, which, in a rough estimation, corresponds to 40−50% filling efficiency in respect to the theoretical limit.

Concerning the formation of the observed well-separated nanoparticles aligned along the inner cavity of the carbon nanotubes (Figure 1), we suggest the following mechanism (Figure 5): (a) The starting materials dissolved in a solvent

dx.doi.org/10.1021/cg400405k | Cryst. Growth Des. 2013, 13, 2707−2710

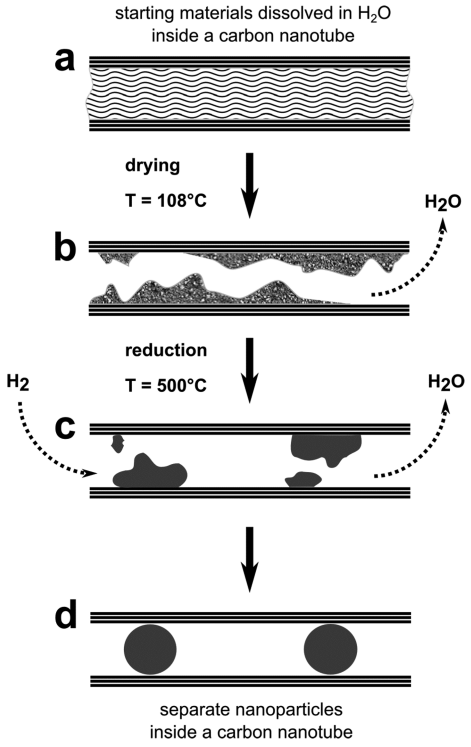

Figure 5. Scheme of the suggested formation mechanism of spherical intermetallic nanoparticles inside carbon nanotubes. The individual steps are (a) carbon nanotube filled with a solvent that carries the starting materials, (b) drying, (c) reduction in hydrogen gas stream, and (d) the completed formation of spherical particles.

enter the inner cavity of the nanotube. (b) During the drying of the solvent-filled nanotubes, water exits the nanotubes and oxides remain on the inner walls of the carbon nanotubes and the overall volume of the filling is largely reduced. (c) During the reduction process, hydrogen reduces the oxides to metals and exits the tubes in the form of water. Again, the volume of the filling is reduced. Since metals usually do not wet the carbon nanotubes,[15] the contact area between metal and carbon nanotube tends to minimize. Hence, at elevated temperature the metal filling at the walls agglomerates and (d) forms spherical particles. Since after step (c) the filling constitutes only a small fraction of the inner volume, the formed particles are well-separated by "empty" regions of the carbon nanotube. Experimentally, we can verify the presence of oxides inside the nanotubes after the drying step, as well as the presence of spherically intermetallic nanoparticles and absence of oxides after the reduction. The in situ observation of the intermediate steps constitutes a challenge, which will be an object of future research.

With energy dispersive X-ray analysis (EDX), we were able to confirm the expected 2:1:1 stoichiometry of the Heusler nanoparticles. We applied a dual approach: averaging over a larger amount, (corresponding to an analyzed area of approximately $1 \times 1\ \mu m^2$), of filled carbon nanotubes with SEM-EDX and single-particle EDX in TEM on numerous individual particles. Both approaches (i.e., averaging over a large number of particles and measuring individual particles) give comparable results and are in good agreement with the Heusler-typical 2:1:1 stoichiometry of Co_2FeGa within the experimental error.

TEM-based nanobeam electron diffraction carried out on individual Heusler nanoparticles reveals that the filling particles are single crystalline (Figure 6). We observe the Heusler-typical

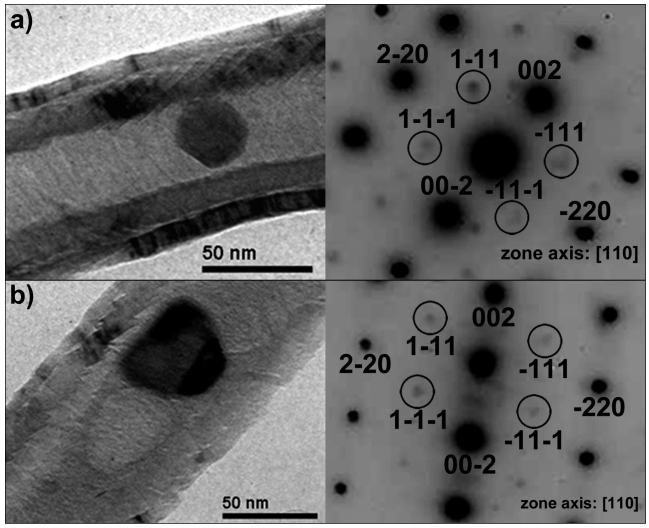

Figure 6. Bright field TEM images and corresponding nanobeam diffraction patterns of individual Co_2FeGa particles inside carbon nanotubes as observed from a [110] zone axis. The diffraction patterns and, in particular, the presence of the 111 and 200 superstructure reflections are evidence for the single crystalline character and a high degree of structural order of the filling particles.

$L2_1$ lattice structure, as indicated by the superstructure reflections corresponding to the 111 and 200 lattice planes, which coincides with the bulk one, giving evidence for a high structural integrity of the filling particles. The $L2_1$ structure of the Heusler nanoparticles points to an absence of atomic site disorder within the filling particles, which we attribute to the moderate temperatures applied during synthesis. Hence, our synthesis approach may constitute a promising way to produce Heusler materials with high crystalline integrity, while suppressing atomic site disorder.

In order to investigate the physical effects of downsizing, we exemplarily studied the magnetic properties of the encapsulated Heusler nanoparticles by performing field- and temperature-dependent measurements of the magnetization (Figure 7). The saturation magnetic moment is $m_S = 4.5 \pm 0.6\ \mu B$/f.u., a value which is comparable to the experimental values reported for Co_2FeGa bulk samples ($4.72\ \mu B$/f.u. $\leq m_{S,exp} \leq 5.15\ \mu B$/f.u.).[16−18] The temperature dependence shows that the saturation magnetization of the sample changes less than 5% when going from 5 to 300 K. The weak decrease of the magnetic moment with rising temperature in the above-mentioned temperature range correlates with the known high T_C for bulk Co_2FeGa[15,16] and indicates that two important magnetic properties of the bulk material, the large saturation magnetization and high critical temperature, are preserved in the Heusler nanoparticles. This result is contrasted by a pronounced concomitant change in magnetic hardness. The measured coercive field of the Co_2FeGa nanoparticles is $H_C = 46.6 \pm 0.7$ kA/m (approximately 585 Oe), which is more than a factor of 30 larger than the measured coercive field $H_C = 1.5$ kA/m (approximately 19 Oe) of a polycrystalline bulk Co_2FeGa reference sample, which had been prepared from elemental metals by the use of the arc-melting technique, as described elsewhere.[19] The large enhancement of the coercive

dx.doi.org/10.1021/cg400405k | Cryst. Growth Des. 2013, 13, 2707−2710

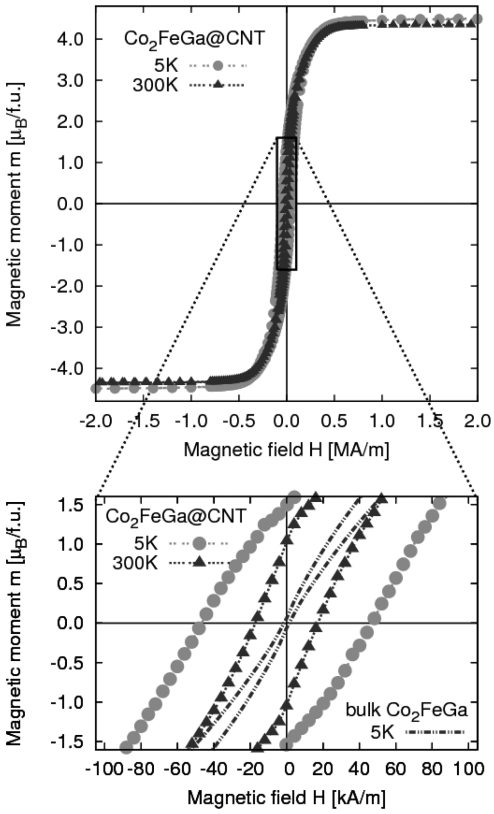

Figure 7. Hysteresis curves of carbon nanotubes filled with Co_2FeGa Heusler nanoparticles measured at 5 K and 300 K. The lower panel shows an enlarged view on the hysteresis curve in comparison with a polycrystalline bulk sample. Here, the enhanced coercive field in Heusler-filled carbon nanotubes can be clearly identified.

field observed in Co_2FeGa nanoparticles can be explained by a transition from a multidomain to a single-domain state in nanoparticles.[20,21] The altered magnetic hardness results in the ferromagnetic and not yet superparamagnetic character of the nanoparticles at room temperature, as is clearly seen from the measured hysteresis loops at 5 K and at 300 K.

In summary, our study demonstrates that a wet chemical method based on filling carbon nanotubes with nitrate solutions offers a facile way to synthesize ternary intermetallic nanoparticles in a well-defined manner. We exemplarily observed altered magnetic properties of Co_2FeGa nanoparticles due to size reduction of the material. Our approach opens the perspective of investigating the properties of not only Heusler compounds but also numerous other intermetallic materials in the form of chemically stable and spherical nanoparticles with well-defined dimensions. The here reported synthesis approach may constitute an exceptional way not only to synthesize single crystalline Heusler (nano)materials with low atomic site disorder but also to scale a given intermetallic compound down to nanosize.

■ ASSOCIATED CONTENT

Supporting Information

Experimental and measurement details. This material is available free of charge via the Internet at http://pubs.acs.org.

■ AUTHOR INFORMATION

Corresponding Author

*(S.H.) E-mail: s.hampel@ifw-dresden.de. (S.W.) E-mail: s.wurmehl@ifw-dresden.de.

Notes

The authors declare no competing financial interest.

■ ACKNOWLEDGMENTS

We thank G. Kreutzer, S. Gaß, T. Gemming, J. Thomas, and A. Wolter for support. We express our gratitude to the DFG for funding in the Emmy Noether Programm under Grant WU595/3-1. M.G. acknowledges support from the Studienstiftung des deutschen Volkes; M.D. thanks the Deutscher Akademischer Austauschdienst (DAAD), and S.H. acknowledges the Bundesministerium für Bildung und Forschung (BMBF) for funding within the program Carbometal under Grant FKZ03X0057D.

■ REFERENCES

(1) Heusler, F. *Verh. Dtsch. Phys. Ges.* **1903**, *5*, 219.
(2) Heusler, F.; Starck, W.; Haupt, E. *Verh. Dtsch. Phys. Ges.* **1903**, *5*, 220−223.
(3) Graf, T.; Felser, C.; Parkin, S. S. P. *Prog. Solid State Chem.* **2011**, *39*, 1−50.
(4) Felser, C.; Fecher, G. H.; Balke, B. *Angew. Chem., Int. Ed.* **2007**, *46*, 668−699.
(5) Javey, A.; Guo, J.; Paulsson, M.; Wang, Q.; Mann, D.; Lundstrom, M.; Dai, H. *Phys. Rev. Lett.* **2004**, *92*, 106804.
(6) Wilcoxon, J. P.; Martin, J. E.; Parsapour, F.; Wiedenman, B.; Kelley, D. F. *J. Chem. Phys.* **1998**, *108*, 9137−9143.
(7) Didier, A.; Lu, F.; Aranzaes, J. R. *Angew. Chem., Int. Ed.* **2005**, *44*, 7852−7872.
(8) Wang, Y. D.; Ren, Y.; Nie, Z. H.; Liu, D. M.; Zuo, L.; Choo, H.; Li, H.; Liaw, P. K.; Yan, J. Q.; McQueeney.; et al. *J. Appl. Phys.* **2007**, *101*, 063530.
(9) Vinesh, A.; Bhargava, H.; Lakshmi, N.; Venugopalan, K. *J. Appl. Phys.* **2009**, *105*, 07A309.
(10) Vallal Peruman, K.; Mahedran, M.; Seenithurai, S.; Chokkalingam, R.; Singh, R. K.; Chandrasekaran, V. *J. Phys. Chem. Solids* **2010**, *7*, 1540−1544.
(11) Basit, L.; Wang, C.; Jenkins, C. A.; Balke, B.; Ksenofontov, V.; Fecher, G. H.; Felser, C.; Mugnaioli, E.; Kolb, U.; Nepijko, S. A.; et al. *J. Phys. D: Appl. Phys.* **2009**, *42*, 084018.
(12) Tsang, S. C.; Chen, Y. K.; Harris, P. J. F.; Green, M. L. H. *Nature* **1994**, *372*, 159−162.
(13) Elmers, H. J.; Fecher, G. H.; Valdaitsev, D.; Nepijko, S. A.; Gloskovskii, A.; Jakob, G.; Schönhense, G.; Wurmehl, S.; Block, T.; Felser.; et al. *Phys. Rev. B* **2003**, *67*, 104412.
(14) Wurmehl, S.; Martins Alves, M. C.; Morais, J.; Ksenofontov, V.; Teixeira, S. R.; Machado, G.; Fecher, G. H.; Felser, C. *J. Phys. D: Appl. Phys.* **2007**, *40*, 1524−1533.
(15) Dujardin, E.; Ebbesen, T. W.; Hiura, H.; Tanigaki, K. *Science* **1994**, *265*, 1850−1852.
(16) Brown, P. J.; Neumann, K. U.; Webster, P. J.; Ziebeck, K. R. A. *J. Phys.: Condens. Matter* **2000**, *12*, 1827−1835.
(17) Deb, A.; Itou, M.; Sakurai, Y.; Hiraoka, N.; Sakai, N. *Phys. Rev. B* **2001**, *63*, 064409.
(18) Chen, P.; Wu, G. H.; Zhang, X. X. *J. Alloys Compd.* **2008**, *454*, 52−56.
(19) Wurmehl, S.; Fecher, G. H.; Kandpal, H. C.; Ksenofontonov, V.; Felser, C.; Lin, H.-J.; Morais, J. *Phys. Rev. B* **2005**, *72*, 184434.
(20) Kneller, E. F.; Luborsky, F. E. *J. Appl. Phys.* **1963**, *34*, 656−658.
(21) Cullity, B. D.; Graham, C. D. In *Introduction to Magnetic Materials*; John Wiley and Sons: Hoboken, NJ, 2009; Chapter 11, pp 360−364.